Computational Materials Science 77 (2013) 161–171

Contents lists available at SciVerse ScienceDirect

Computational Materials Science

journal homepage: www.elsevier.com/locate/commatsci

Innovative coupled fluid–structure interaction model for carbon nano-tubes conveying fluid by considering the size effects of nano-flow and nano-structure

Mehran Mirramezani, Hamid Reza Mirdamadi *, Mostafa Ghayour

Department of Mechanical Engineering, Isfahan University of Technology, 84156-83111 Isfahan, Iran

ARTICLE INFO

Article history:
Received 20 February 2013
Received in revised form 8 April 2013
Accepted 16 April 2013
Available online 18 May 2013

Keywords:
Fluid–structure interaction (FSI)
Divergence instability
Critical flow velocity
Knudsen number
Viscosity parameter
Size-dependent continuum theory

ABSTRACT

In this article, we reappraise the well-known equation of motion for a pipe conveying viscous fluid. We utilize prominent principles of fluid mechanics such as Navier–Stokes' equation as well as several benchmark references in the field of fluid–structure interaction (FSI) to reveal that the viscosity of the fluid flow should not appear explicitly in the equation of motion of pipe conveying fluid. Based on this result, we could develop an innovative model for one dimensional coupled vibrations of carbon nano-tubes (CNTs) conveying fluid using slip velocity of the fluid flow on the CNT walls as well as utilizing size-dependent continuum theories to consider the size effects of nano-flow and nano-structure. Therefore, this innovative coupled FSI equation suggests that CNTs conveying nano-flow remain stable for higher velocities. In the other words, the critical average velocity of the fluid flow at which the divergence instability occurs, should be greater in comparison with the critical velocity predicted by the models used plug flow and classical continuum theories.

1. Introduction

Carbon nano-tubes (CNTs) are becoming the most promising material for nano-electronics, nano-devices and nano-composites because of their enormous application such as nano-pipettes, actuators, reactors, fluid filtration devices, biomimetic selective transport of ions, targeted drug delivery devices, scanning molecule microscopy, and scanning ion conductance microscopy [1–4]. In this regard, a remarkable number of studies have been accomplished to disclose the vibrational behavior of such nano-structures conveying fluid. Tuzun et al. [5], Amabili et al. [6], Yoon et al. [7], Natsuki et al. [8], Wang et al. [9], Xia et al. [10] and Wang and Qiao [11] made important contributions in this practical area. In this research, we would undertake a reevaluation for computational modeling of carbon nano-tubes conveying viscous fluid with some fresh insights as well as we try to develop an innovative one dimensional (1D) coupled fluid–structure interaction (FSI) equation by considering slip condition on the nano-tube wall. Khosravian and Rafii Tabar [12] studied the flow of viscous fluid through a carbon nano-tube and established a new equation of motion of pipe conveying fluid by considering the viscosity effect. They found that a nano-tube conveying a viscous fluid was more stable against vibration-induced buckling than a nano-tube conveying a non-viscous fluid. Wang and Ni [13] reappraised the computational modeling of carbon nano-tube conveying viscous fluid represented by Khosravian and Rafii Tabar [12] and then corrected the FSI equation and disclosed that the effect of viscosity of fluid flow on the vibration and instability of CNTs could be ignored. Lee and Chang [14] analyzed the influences of nonlocal effect, viscosity effect, aspect ratio, and elastic medium constant on the fundamental frequency of a single-walled carbon nano-tube (SWCNT) conveying viscous fluid embedded in an elastic medium. They revealed that the frequency increased as the values of the viscosity parameter increased. Soltani et al. [15] developed a transverse vibrational model for a viscous fluid-conveying SWCNT embedded in biological soft tissue. Their investigation determined that the structural instability and the associated critical flow velocity could be affected by the viscosity of the fluid and the nonlocal parameter. Khoddami et al. [16] studied electro-thermo nonlinear vibration and instability of embedded double-walled Boron Nitride nano-tubes (DWBNNTs) conveying viscous fluid based on nonlocal piezoelasticity theory. They reported that increasing the small scale parameter decreased the real and imaginary parts of frequency and critical fluid velocity. Furthermore, they concluded that the effect of fluid viscosity on the vibration and instability of DWBNNTs might be ignored. In many recent studies various size-dependent continuum theories have been developed for vibration and stability analysis of CNTs conveying fluid. Lee and Chang [17], Zhen

* Corresponding author. Tel.: +98 311 391 5248; fax: +98 311 391 2628.
E-mail addresses: m.mirramezani@me.iut.ac.ir (M. Mirramezani), hrmirdamadi@cc.iut.ac.ir (H.R. Mirdamadi), ghayour@cc.iut.ac.ir (M. Ghayour).

0927-0256/$ - see front matter © 2013 Elsevier B.V. All rights reserved.
http://dx.doi.org/10.1016/j.commatsci.2013.04.047

and Fang [18], Jannesari et al. [19] included the effect of small-size into equations of motion by using nonlocal elasticity in their studies and showed that increasing nonlocal parameter had the effect of a decrease in the critical velocity of fluid. Ke and Wang [20] investigated vibration and instability of fluid-conveying double-walled carbon nano-tubes based on modified couple stress theory. They showed that the imaginary component of the frequency and the critical flow velocity of the CNTs increased with an increase in length scale parameter. Wang [21] developed a theoretical analysis of wave propagation of fluid-conveying single-walled carbon nano-tubes based on strain gradient elasticity theory. He showed that the use of gradient elasticity theory had a dramatic effect on dispersion relation. Wang [22] utilized nonlocal elasticity theory integrated with surface elasticity theory to analyze dynamic response of nano-tubes conveying fluid. He revealed that fundamental frequency and critical flow velocity predicted by his new model was generally higher than that predicted by the Euler–Bernoulli beam model without surface effects. Some recent studies developed to consider the small size effects of nano-flow as well as slip boundary condition on nano-tube wall. For instance, Rashidi et al. [23] presented an original model for a single-mode coupled vibrations of nano-tubes conveying fluid by considering the slip boundary conditions of nano-flow quantified by Knudsen number (*Kn*). They reported, for the passage of gas through a nano-pipe with nonzero *Kn*, that the critical flow velocities could decrease considerably in comparison with a liquid nano-flow. Mirramezani and Mirdamadi [24] investigated coupled-mode flutter stability of nano-tube conveying gas and liquid nano-flow for different beam boundary conditions and multi-mode analysis. They observed that coupled-mode flutter might occur much sooner by considering slip condition than that predicted by continuum theory. Kaviani and Mirdamadi [25] studied the wave propagation phenomena in CNT conveying fluid. The CNT structure was modeled by using size-dependent strain/inertia gradient theory of continuum mechanics, the CNT wall-fluid interaction by slip boundary condition and Knudsen number (*Kn*). They reported that *Kn* could impress complex wave frequencies at both lower and higher ranges of wave numbers, while the small-size had impression at the higher range. Mirramezani and Mirdamadi [26] investigated the effect of nano-size of both fluid flow and elastic structure simultaneously on the vibrational behavior of a nano-tube conveying fluid using both *Kn* and nonlocal continuum theory. It was observed that the nonlocal parameter would have more effect than *Kn* on the reduction of critical velocities of a liquid nano-flow. This effect had considerable impact on the reduction of critical velocities for a clamped–clamped beam in comparison with a pinned–pinned one. Kaviani and Mirdamadi [27] considered the coupled effects of *Kn* and slip boundary condition on the viscosity of a nano-flow passing through a nano-tube. *Kn*-dependent viscosity could affect both directly on viscosity values and indirectly on a dimensionless parameter, velocity correction factor, VCF, defined as the ratio of no-slip flow velocity to slip flow velocity on the boundaries of a nano-tube. They concluded that the effect of viscosity on the critical flow velocity could be so large that for a specific numerical study could reach one-fourth of that velocity, by ignoring the viscosity effect on slip boundary condition. Matin et al. [28] studied the effects of nonlocal elasticity and slip condition on vibration of nano-plate coupled with fluid flow. They reported that the effect of nonlocal parameter would be considerable for plate lengths less than 50 nm as well as when the fluid is a liquid, most of the contribution in decreasing critical flow velocity is due to nonlocal parameter but when the fluid is a gas, *Kn* has a greater role in decreasing the critical velocity.

A partial objective of this study is to reappraise the equation of motion of pipe conveying viscous fluid extracted by Khosravian and Rafii Tabar [12]. In this article, we utilize basic principles of fluid mechanics such as Navier–Stokes' equation; moreover, we benefit from some valuable classical works in the field of FSI to reveal that the viscosity of the fluid flow should not appear explicitly in the equation of motion. Furthermore, we propose a novel model, for 1D coupled vibrations of carbon nano-tubes (CNTs) conveying fluid, taking into account the slip boundary condition using Knudsen number as well as size-dependent continuum theories such as strain/inertia gradient and nonlocal theories. It could be seen that the current model by considering the size effects of nano-flow and nano-structure, the critical mean flow velocity at which the divergence-type instability might occur, could differ remarkably from that of a plug flow model for the fluid flow.

The remainder of this study is organized as follows: In Section 2, we reappraise the equation of motion of pipe conveying viscous fluid. In Section 3, we develop an innovative 1D coupled FSI equation by considering slip condition and size-dependent continuum theories. In Section 4, we implement the Galerkin weighted-residual solution technique and solve the partial differential equations of nano-tube vibrations. In Section 5, we discuss stability analysis and present the results. Finally, in Section 6, we express our conclusions.

2. Reappraise the equation of motion of pipe conveying viscous fluid

The flexural vibrations of an Euler–Bernoulli beam subjected to an external force can be modeled via the following equation [29]:

$$-\frac{\partial^2 M}{\partial x^2}+m_c\frac{\partial^2 W}{\partial t^2}=F_{ext} \tag{1}$$

where x is the longitudinal coordinate of tube elastic axis; m_c, the CNT mass per unit length; W is the flexural displacement of the CNT wall; t, time; F_{ext} is the transversal external force acting on the beam due to the flowing fluid and M is the bending moment. The bending moment for an Euler–Bernoulli beam is given by:

$$M=-EI\frac{\partial^2 W}{\partial x^2} \tag{2}$$

where E is Young's modulus and I is the moment of inertia of area cross section. In the following part of this section, we benefit from the well-known Navier–Stokes' equation to compute the F_{ext} exerted by the fluid flow on the wall of CNT conveying viscous fluid.

2.1. A brief review on fluid mechanics

We consider an incompressible, laminar, infinite and viscous fluid flowing through the CNT. The momentum-balance equation for the fluid motion may be described by the well-known Navier–Stokes' equation as [30]:

$$\rho\frac{D\vec{V}}{Dt}=-\nabla\vec{P}+\mu\nabla^2\vec{V}+\vec{F}_{body} \tag{3}$$

where D/Dt is the material or total derivative and $\vec{V}$ is the flow velocity, $\vec{P}$ and μ are, respectively, the pressure and the viscosity of the flowing fluid, ρ is the mass density of the internal fluid, and $\vec{F}_{body}$ represents body forces. The body forces are due to external fields like gravity, magnetism an electric potential, which would act upon the entire mass within the body. We neglect these effects and ignore the body forces. In the following equations, we concentrate on how to compute the F_{ext} exerted by the fluid flow on the wall of CNT conveying viscous fluid using basic principles of fluid mechanics to modify the equation of motion extracted by Refs. [12,13]. According to the reference [30] the total force exerted on the differential element of the fluid in each direction can be com-

puted by the differential equation describing the linear momentum of the fluid flow as follows:

$$d\vec{F} = \rho \frac{D\vec{V}}{Dt} dxdydz \tag{4}$$

It is noted that this is a vector relation and shows that the resultant force in each direction is obtained from multiplying the mass element by the material derivative of velocity vector in that direction. The force resultants on the differential element of the fluid are of two types, body forces and surface forces. The only body force considered in this study is the gravitational force exerted on the differential mass within the control volume, which is defined as follows [30]:

$$d\vec{F}_{gravity} = \rho \vec{g}\, dxdydz \tag{5}$$

The surface forces are due to the stresses exerted on the sides of the control surface. For example, the net surface force along the z direction is given by [30]:

$$dF_{z,surf} = \left(\frac{\partial}{\partial x}(\sigma_{xz}) + \frac{\partial}{\partial y}(\sigma_{yz}) + \frac{\partial}{\partial z}(\sigma_{zz})\right) dxdydz \tag{6}$$

Then we can split down this force into pressure parts plus viscous stresses [30]:

$$dF_{z,surf} = \left(-\frac{\partial P}{\partial z} + \frac{\partial}{\partial x}(\tau_{xz}) + \frac{\partial}{\partial y}(\tau_{yz}) + \frac{\partial}{\partial z}(\tau_{zz})\right) dxdydz \tag{7}$$

Then we could say that [30]:

$$dF_z = \rho g_z dxdydz + \left(-\frac{\partial P}{\partial z} + \frac{\partial}{\partial x}(\tau_{xz}) + \frac{\partial}{\partial y}(\tau_{yz}) + \frac{\partial}{\partial z}(\tau_{zz})\right) dxdydz \tag{8}$$

If Eq. (8) is substituted into Eq. (5) and the components of velocity vector along x,y and z directions are denoted by u, v and w respectively, we have along the z direction [30]:

$$\rho\left(\frac{\partial w}{\partial t} + u\frac{\partial w}{\partial x} + v\frac{\partial w}{\partial y} + w\frac{\partial w}{\partial z}\right) = \rho g_z + \left(-\frac{\partial P}{\partial z} + \frac{\partial}{\partial x}(\tau_{xz}) + \frac{\partial}{\partial y}(\tau_{yz}) + \frac{\partial}{\partial z}(\tau_{zz})\right) \tag{9}$$

It should be noted that the effect of viscosity due to the fluid flow appears in Eq. (9) resulting from shear stresses that have a direct relation to viscosity. We conclude from above equations and the linear momentum balance law that the force resultant in each direction could be calculated by the material derivative of the velocity vector in the corresponding direction, or in another way, this force could be similarly calculated by summing the pressure gradient and the viscous stress in that direction. In other words, both the right and left hand sides of Eq. (9) represent the force resultant in the z direction but in two different ways.

2.2. A reappraisal modeling of CNTs conveying viscous fluid

According to the previous brief review of fluid mechanics, from now on we initiate to reappraise the equation of motion of pipe conveying viscous fluid given by references [12,13]. According to Eq. (1) we have to determine F_{ext} exerted by the fluid flow on the walls of CNT conveying viscous fluid in the lateral direction. In this way, we utilize Eq. (3) and we need to determine the velocity vector of the fluid flow. Therefore, the compatibility condition at the point of contact between the nano-tube and the internal fluid would require that their corresponding velocities and accelerations along the direction of flexural displacement become the same. These conditions can then be written as:

$$V_r = \frac{DW}{Dt} \tag{10}$$

and

$$\frac{DV_r}{Dt} = \frac{D^2W}{Dt^2} \tag{11}$$

where

$$\frac{D}{Dt} = \frac{\partial}{\partial t} + V_x(r)\frac{\partial}{\partial x} \tag{12}$$

It should be noticed that due to applying a compatibility condition on the CNT wall, $V_x(r)$ is the velocity of the fluid flow on the CNT wall. By using Eqs. (10)–(12) and substituting them into the left hand side of Eq. (3) as well as multiplying all the terms by the cross sectional area of the internal fluid, A_i, we could reach to the following equation:

$$\rho A_i \frac{DV_r}{Dt} = \rho A_i \left(2V_x(r)\frac{\partial^2 W}{\partial x \partial t} + V_x(r)^2 \frac{\partial^2 W}{\partial x^2} + \frac{\partial^2 W}{\partial t^2}\right) \tag{13}$$

and the right hand side of Eq. (3) by considering a cylindrical coordinates as well as replacing z by r, can be computed as:

$$A_i\left(-\frac{\partial P}{\partial z} + \frac{\partial}{\partial x}(\tau_{xz}) + \frac{\partial}{\partial y}(\tau_{yz}) + \frac{\partial}{\partial z}(\tau_{zz})\right) = -A_i\frac{\partial P_r}{\partial r} + \mu A_i\left(\frac{\partial^3 W}{\partial x^2 \partial t} + V_x(r)\frac{\partial^3 W}{\partial x^3}\right) \tag{14}$$

Now we can rewrite the momentum-balance equation for the Newtonian fluid motion in the lateral direction as follows:

$$F_z = -A_i\frac{\partial P_r}{\partial r} + A_i\mu\left(\frac{\partial^3 W}{\partial x^2 \partial t} + V_x(r)\frac{\partial^3 W}{\partial x^3}\right) = \rho A_i\left(2V_x(r)\frac{\partial^2 W}{\partial x \partial t} + V_x(r)^2\frac{\partial^2 W}{\partial x^2} + \frac{\partial^2 W}{\partial t^2}\right) \tag{15}$$

According to the previous discussion about momentum-balance equation, it should be noticed that both Eqs. (13) and (14) represent the net force acting on the fluid element in the lateral direction in the same way. It would rather be declared that Eq. (13) would represent the net force generated by lateral acceleration of CNT and the longitudinal velocity of the fluid flow; while Eq. (14) could represent the same force by the pressure gradient and viscosity of the flowing fluid. We could use Eq. (13) or Eq. (14) interchangeably representing $-F_{ext}$ in Eq. (1), because the forces acting between a fluid element and a neighboring CNT wall could be implemented as action and reaction forces in opposite directions. Consequently, the equation of motion of CNT conveying viscous fluid can be written as:

$$EI\frac{\partial^4 W}{\partial x^4} + m_c\frac{\partial^2 W}{\partial t^2} + m_f\left(2V_x(r)\frac{\partial^2 W}{\partial x \partial t} + V_x(r)^2\frac{\partial^2 W}{\partial x^2} + \frac{\partial^2 W}{\partial t^2}\right) = 0 \tag{16}$$

where ρA_i is replaced by the fluid mass per unit length, $m_f$and $V_x(r)$ is the velocity of the fluid flow in the longitudinal direction on the CNT wall. If we would consider a plug flow in a pipe conveying fluid, then the velocity of the fluid flow should be uniform at each cross section and equal to the mean flow velocity; consequently, Eq. (16) should be exactly similar to the well-known FSI equation derived by Paidoussis [31]. Eq. (16), which is defining the vibrational characteristic of a pipe conveying viscous fluid, would seem different from the equation of motion of pipe conveying viscous fluid extracted in Refs. [12,13] and by now, used by several researchers. This equation was derived as follows [13]:

$$EI\frac{\partial^4 W}{\partial x^4}+m_c\frac{\partial^2 W}{\partial t^2}+m_f\left(2V_x(r)\frac{\partial^2 W}{\partial x\partial t}+V_x(r)^2\frac{\partial^2 W}{\partial x^2}+\frac{\partial^2 W}{\partial t^2}\right)-A_i\mu\left(\frac{\partial^3 W}{\partial x^2\partial t}+V_x(r)\frac{\partial^3 W}{\partial x^3}\right)=0 \quad (17)$$

We believe that the viscosity parameter could not appear in the FSI equation. There are major reasons as discussed in the following paragraphs. In the procedure followed by references [12,13], the authors investigated that $A_i(\partial P_r/\partial r)$ is the force acting in the direction of the flexural displacement due to fluid flow. However, we are convinced that this expression should be modified and this would be the main reason of appearing the viscosity parameter in the equation of motion. According to the previous discussion about Navier–Stokes' equation as well as Eq. (15), we conclude that the force due to fluid flow in the lateral direction could be calculated by summing pressure gradient and shear stresses due to viscosity, which are equal to $-A_i(\partial P_r/\partial r)+A_i\mu(\partial^3 W/\partial x^2\partial t+V_x(r)(\partial^3 W/\partial x^3))$; however, the authors of the references [12,13] used only the pressure gradient as a lateral force. Therefore, they observed the viscosity effects on the other side of Eq. (15) and it is the main reason of appearing viscosity parameter in the equation. We could verify our results by reference [31]. Paidoussis [30] derived the linear equation of motion for a pipe conveying fluid by the both Newtonian and the Hamiltonian approaches. In this study, we use his Newtonian approach. The free body diagram of pipe and fluid element are plotted as Fig. 1 [31].

We observe in reference [31] that the fluid element is subjected to various forces such as: (1) Pressure forces, where the pressure (P) because of frictional losses; (2) reaction forces of the pipe on the fluid normal to the fluid element, $F\delta s$, and tangential to it, $qS\delta s$, associated with the wall shear stress; and (3) gravity forces $Mg\delta s$ in the x direction.

The term $qS\delta s$ is due to shear stress of fluid flow and this shear stress is because of viscosity of the fluid flow. From this term we may conclude that Paidoussis [31] considered the effect of viscosity of the fluid flow to derive the governing equation of motion. If we follow his procedure to realize the resulting equation of motion for FSI, we find that this term disappeared because it is an internal force. In fact, if the pipe and the fluid conveyed are taken as a free body, the frictional forces exchanged between them are acting as internal forces, and hence they should not appear in the resulting equation of motion. Moreover, Paidoussis emphasized in his different publications [32,33] that "It should be stressed that the absence of viscous flow terms in the well-known FSI equation does not signify that the model is inviscid; it is indeed based on a 1D viscous flow model". Guo et al. [34], focusing on the effects of fluid viscosity on the governing equation of motion of pipes conveying fluid and on the critical velocities for both divergence and flutter, would confirm our previous results. It is noted that the viscosity of the fluid may have two different effects on the FSI equation: (i) the friction between the fluid and the pipe wall and (ii) the non-uniformity of flow velocity distribution across the cross-section. The first effect was noted and accounted for by Benjamin [35] and was later elaborated upon by Paidoussis [31]. From their articles we may conclude that the shear traction over the pipe and pressure-loss due to viscosity exactly cancel out, and hence they should not explicitly appear in the FSI equation.

Finally, according to our investigation about how to exert the F_{ext} into the equation of flexural vibration of an Euler–Bernoulli beam and discussion quoted by several references [31–35], we may conclude that Eq. (16) should be valid for viscous and non-viscous fluid flow. In the following section we try to develop an innovative 1D coupled FSI equation by considering slip condition on the pipe walls and we will reveal a considerable change in the first divergence critical flow velocity in comparison with plug flow theory.

3. Innovative 1D coupled FSI equation by considering size effects

3.1. Size effect of nano-flow

Regarding the procedure we utilized to calculate theF_{ext}, we could benefit from the compatibility condition at the point of contact between the CNT and the internal fluid to determine the velocity of the fluid flow. Due to applying a material derivative at a contact point of the fluid and CNT wall, it would be logical that the $V_x(r)$ appearing in the previous equation should be the velocity of the fluid flow along the longitudinal direction touching the CNT wall [12]. The no-slip condition corresponding $V_x(r)=0$, would be applied to the walls of the nano-tube as a result of the viscosity of the fluid and consequently, this would imply that the two related terms in Eq. (16) should vanish. If we consider a plug flow theory, $V_x(r)$ would be equal to a mean flow velocity of the fluid flow at each section and then we have the plug flow-based FSI equation. Another way is to consider a slip condition at the CNT wall which could be an acceptable idea for a nano-flow. The Knudsen number (Kn), i.e., the dimensionless ratio of the mean free path

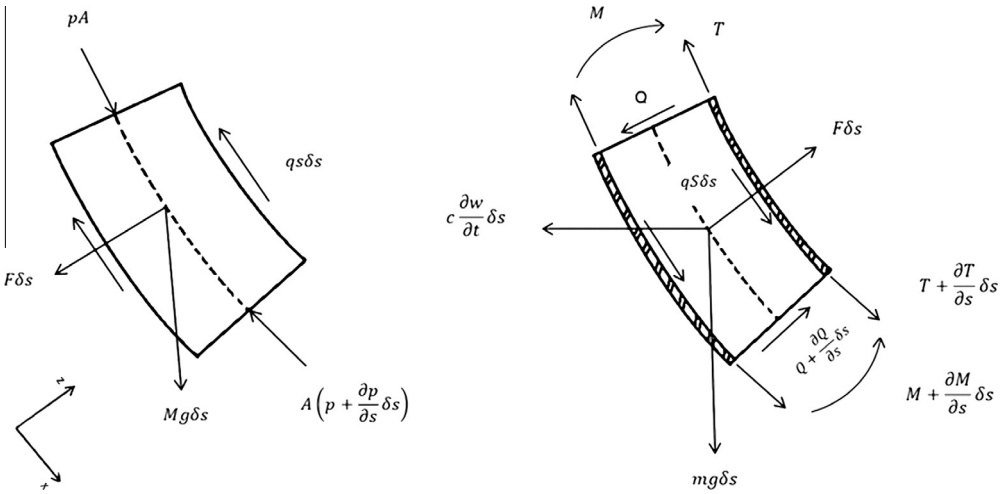

Fig. 1. Forces acting on an element of the fluid (left side); forces and moments on the corresponding element of the pipe (right side).

of the fluid molecules to a characteristic length of the flow geometry, is used as a discriminant for identifying the different flow regimes [35]. Based on Kn, four flow regimes may be identified and for $10^{-2} < Kn < 0.1$ the slip flow regime could be considered [36]. For CNTs conveying fluid, the Kn may be larger than 10^{-2}; consequently, the assumption of no-slip boundary condition should be no longer valid. Beskok and Karniadakis [37] proposed a formulation for a slip velocity model, which is claimed to be rather a more representative relation for correlating to the experimental data:

$$V_s - V_w = \left(\frac{2-\sigma_v}{\sigma_v}\right)\left(\frac{Kn}{1-bKn}\right)\left(\frac{\partial V}{\partial n}\right)_{r=R} \tag{18}$$

where b is a general slip coefficient. By choosing $b = -1$, one can make the effect of slip condition as accurate as a second-order term [37]. V_s is the slip velocity of the fluid near the CNT wall surface, V_w is the axial velocity of the solid wall as a rigid body and n is an outward unit vector normal to the CNT wall surface. σ_v is tangential momentum accommodation coefficient and is considered to be 0.7 for most practical purposes [38]. The solution of Navier–Stokes' equation in the axial direction of an orthogonal cylindrical coordinate system for a pipe is as follows [30]:

$$V = \frac{1}{4\mu}\left(\frac{\partial P}{\partial x}\right)r^2 + C \tag{19}$$

where r and x are, respectively, the radial and longitudinal coordinates of both the tube elastic axis and the axial flow, and P is the pressure. By considering $V_w = 0$ and replacing $(\partial V/\partial n)_{r=R}$ by $-R \times (\partial V/\partial\ r)_{r=R}$ in Eq. (18), and computing $(\partial V/\partial r)_{r=R}$ from Eq. (19), we could rewrite the slip velocity at the CNT wall as:

$$V_s = -\frac{R^2}{2\mu}\left(\frac{\partial P}{\partial x}\right)\left[\left(\frac{2-\sigma_v}{\sigma_v}\right)\left(\frac{Kn}{1+Kn}\right)\right] \tag{20}$$

where R is the inner radius of the tube. Due to a tendency for eliminating the dependency of Eq. (20) to the pressure gradient, we need to calculate the mean flow velocity. Therefore, if we consider the slip velocity at the wall of nano-tube for calculating the constant C in Eq. (19) and integrate Eq. (19) over the cross sectional area of the pipe, the average flow velocity is as follows:

$$V_{avg} = -\frac{R^2}{8\mu}\left(\frac{\partial P}{\partial x}\right)\left[1 + 4\left(\frac{2-\sigma_v}{\sigma_v}\right)\left(\frac{Kn}{1+Kn}\right)\right] \tag{21}$$

For simplicity of the following equations, we define a new parameter as:

$$\gamma \triangleq 4\left(\frac{2-\sigma_v}{\sigma_v}\right)\left(\frac{Kn}{1+Kn}\right) \tag{22}$$

If we compute the pressure gradient from Eq. (21) and replace it into Eq. (20), we can rewrite the slip velocity as follows:

$$V_s = \frac{\gamma}{1+\gamma}V_{avg} \tag{23}$$

By substituting Eq. (23) as $V_x(r)$ into Eq. (16), the 1D coupled FSI equation of motion for CNT conveying fluid can be expressed as:

$$EI\frac{\partial^4 W}{\partial x^4} + (m_c + m_f)\frac{\partial^2 W}{\partial t^2} + 2m_f\left(\frac{\gamma}{1+\gamma}\right)V_{avg}\frac{\partial^2 W}{\partial x \partial t} + m_f\left(\frac{\gamma}{1+\gamma}\right)^2 V_{avg}^2\frac{\partial^2 W}{\partial x^2} = 0 \tag{24}$$

To the best of authors' knowledge, Eq. (24) should be an innovative analytical approach to take into account a 1D coupled FSI equation by considering the nano-size effect of nano-flow which is more accurate than considering a plug flow for the nano fluid flow. It should be noted that if the no-slip condition corresponding $Kn = 0$, this would imply that the parameter $\gamma/(1+\gamma)$ is equal to zero and consequently two related terms in Eq. (24) should vanish; therefore, Eq. (24) should be valid just in a slip regime where $Kn \geqslant 0.001$. As we would observe from Fig. 2, if the value of Kn could increase significantly, the slip velocity of the fluid flow on the CNT walls become greater and the profile of the velocity distribution becomes uniform in the cross sectional area of the pipe and the corresponding parameter $\gamma/(1+\gamma)$ become equal to one. Consequently, we approach a plug flow theory and the critical flow velocity approaches the value predicted by plug flow theory which is π.

3.2. Size effect of nano-structure

Classical continuum mechanics theories have been used in a wide range of fundamental problems and applications in mechanical engineering. These theories are utilized for scales ranging roughly from millimeters to meter. In the last few years, standard elasticity formulae have also been used to describe mechanical behavior at the nano scale. Experimental evidence and observations with newly developed equipment have suggested that classical continuum theories do not suffice for an accurate study of the corresponding mechanical phenomena. The inability of classical continuum mechanics theories would because of the lack of an internal length for characterizing the underlying nano-structure from the constitutive equations. Consequently, several researchers during 19th century devoted their attention to enrich the classical continuum theories by considering internal characteristic lengths for nano-structures and they could succeed in developing novel non-classical continuum mechanics for investigating the size-effects in nano-structures. In the following subsections of this article, we would utilize different gradient elasticity formalisms.

3.2.1. Strain/inertia gradient theory

In one of the higher-order continuum theories developed by Mindlin [39], the strain energy is considered as a function of the first and second-order gradients of strain tensor. This theory was then reformulated and renamed strain gradient theory by Fleck and Hutchinson [40]. In the strain gradient theory, the strain gradient tensor is decomposed into two parts of a stretch gradient tensor and a rotation gradient tensor. The strain gradient theory has been successfully applied to analyze the static and dynamic mechanical behavior of micro and nano-structures. The strain gradient formalism combined with inertia gradients was introduced by Askes and Aifantis [41] and is described as:

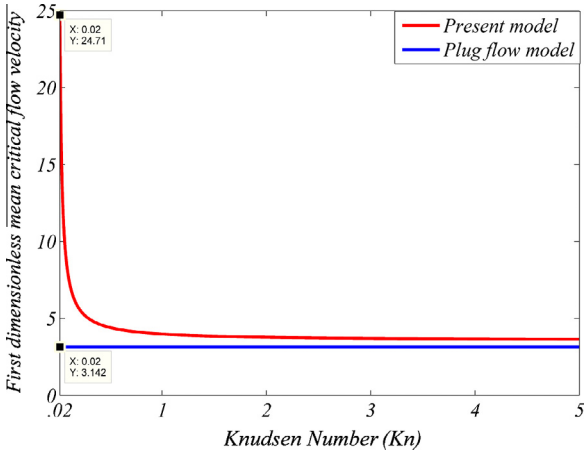

Fig. 2. The variation of the first dimensionless mean critical flow velocity versus Kn for plug flow theory and present model.

$$\rho\left(\ddot{u}_i - l_m^2 \ddot{u}_{i,mm}\right) = C_{ijkl}\left(u_{k,jl} - l_s^2 u_{k,jlmm}\right) \tag{25}$$

where ρ is the mass density of nano-structure, C_{ijkl} are Cartesian components of elasticity tensor and u the denotes displacement. Eq. (25) contains two length scales, l_m and l_s, which are related to the inertia and strain gradients, respectively. The constitutive relation for 1D Euler–Bernoulli beam theory, is obtained by equating $i = 3$ and using the linearized strain–displacement relations of Euler–Bernoulli kinematics. Accordingly, for 1D strain-flexural curvature relation, we have:

$$\varepsilon = -z\frac{\partial^2 W}{\partial x^2} \tag{26}$$

It is found from Eq. (25) that the axial stress in CNTs may be written as:

$$\sigma = E\left(\varepsilon - l_s^2 \frac{\partial^2 \varepsilon}{\partial x^2}\right) + \rho_c l_m^2 \frac{\partial^2 \varepsilon}{\partial t^2} \tag{27}$$

where σ and ε are, respectively, flexural stress and strain in the beam. The bending moment M is given by:

$$M = \int_A z\sigma dA = -EI\left(\frac{\partial^2 W}{\partial x^2} - l_s^2 \frac{\partial^4 W}{\partial x^4}\right) - \rho_c I l_m^2 \frac{\partial^4 W}{\partial x^2 \partial t^2} \tag{28}$$

By substituting the second derivative of Eq. (28) and F_{ext} as calculated in Section 2.2, into Eq. (1), the 1D coupled equation of motion of CNT conveying fluid, considering strain/inertia gradient theory, can be expressed as:

$$EI\left(\frac{\partial^4 W}{\partial x^4} - l_s^2 \frac{\partial^6 W}{\partial x^6}\right) + (m_c + m_f)\frac{\partial^2 W}{\partial t^2} + 2m_f\left(\frac{\gamma}{1+\gamma}\right)V_{avg}\frac{\partial^2 W}{\partial x \partial t} + m_f\left(\frac{\gamma}{1+\gamma}\right)^2 V_{avg}^2 \frac{\partial^2 W}{\partial x^2} + \rho_c I l_m^2 \frac{\partial^6 W}{\partial x^4 \partial t^2} = 0 \tag{29}$$

If we substitute $\gamma/(1+\gamma)$ by one, then Eq. (29) would become the one given by Wang [42].

3.2.2. Stress gradient (nonlocal theory of Eringen)

According to Eringen [43], the nonlocal stress tensor $\sigma^{n.l.}$ at point x is expressed as:

$$\sigma^{n.l.} = \int_V K(|x' - x|, \tau)\sigma^{l.}(x')dx' \tag{30}$$

where $\sigma^{l.}(x)$ is the classical, macroscopic stress tensor at point x and the kernel function $K(|x' - x|, \tau)$ represents the nonlocal modulus, $|x' - x|$ is the distance and τ is the material constant that depends on internal and external characteristic lengths. Eq. (30) represents the weighted average of contribution of the strain field of all points in the body to the stress field at a point. It means that the stress field at a point x in an elastic continuum is dependent not only on the strain field at the point under consideration but also on the strains at all other points of the body. The integral constitutive relation in Eq. (30) makes the elasticity equation difficult to solve. However, it is possible to represent an equivalent differential form as [43]:

$$(1 - l^2\nabla^2)\sigma^{n.l.} = \sigma^{l.} \tag{31}$$

where l is the internal characteristic length and ∇^2 is the Laplacian operator. The relationship between the bending moment resultant and the flexural displacement of the Euler–Bernoulli beam theory, take the following special form [44]:

$$M - l^2\frac{\partial^2 M}{\partial x^2} = -EI\frac{\partial^2 W}{\partial x^2} \tag{32}$$

by substituting $\partial^2 M/\partial x^2$ from Eq. (1) into Eq. (32) we have:

$$M = l^2\left(m_c\frac{\partial^2 W}{\partial t^2} - F_{ext}\right) - EI\frac{\partial^2 W}{\partial x^2} \tag{33}$$

by substituting the second derivative of Eq. (33) and F_{ext} represented in the previous sections into Eq. (1) the 1D FSI equation could be expressed as:

$$EI\frac{\partial^4 W}{\partial x^4} + (m_c + m_f)\frac{\partial^2 W}{\partial t^2} + 2m_f\left(\frac{\gamma}{1+\gamma}\right)V_{avg}\frac{\partial^2 W}{\partial x \partial t} + m_f\left(\frac{\gamma}{1+\gamma}\right)^2 V_{avg}^2\frac{\partial^2 W}{\partial x^2} - l^2\left((m_c + m_f)\frac{\partial^4 W}{\partial x^2 \partial t^2} + 2m_f\left(\frac{\gamma}{1+\gamma}\right)V_{avg}\frac{\partial^4 W}{\partial x^3 \partial t} + m_f\left(\frac{\gamma}{1+\gamma}\right)^2 V_{avg}^2\frac{\partial^4 W}{\partial x^4}\right) = 0 \tag{34}$$

If we choose $\gamma/(1+\gamma)$ equal to one, then Eq. (34) would reduce to those given by Tounsi et al. [45] and Wang [46]. It should be noticed that based on [47,48], in this study we have utilized "partial" nonlocal elasticity, due to ignoring higher-order boundary conditions derived from a variationally consistent formulation, while using nonlocal constitutive law, as a part of equilibrium (static/dynamic), and kinematic (geometric or compatibility) relations. By the same authors, recent trend of nonlocal formulation has been named "exact" nonlocal elasticity, because higher-order terms are derived for both differential equations and boundary conditions of nonlocal boundary value problem. Wang [49] developed the higher-order governing equation and the boundary conditions based on exact nonlocal stress model to examine the vibration properties and stability of nanotubes conveying fluid.

The resultant equation may be rendered dimensionless through the use of dimensionless parameters as:

$$\begin{aligned}
&(a):\tau = \left(\frac{EI}{m_c + m_f}\right)^{\frac{1}{2}}\frac{t}{L^2},\ (b):\zeta = \frac{x}{L},\ (c):\eta = \frac{W}{L},\\
&(d):\beta = \frac{m_f}{m_c + m_f},\ (e):\phi = \frac{l}{L}\\
&(f):U_{avg} = \left(\frac{m_f}{EI}\right)^{\frac{1}{2}}L \times V_{avg}\ (g):\psi = \frac{\rho_c I}{L^2(m_f + m_c)}\\
&(h):\lambda_m = \frac{l_m}{L}\ (f):\lambda_s = \frac{l_s}{L}
\end{aligned} \tag{35}$$

The dimensionless equation by considering the strain/inertia gradient and slip condition is as follows:

$$\frac{\partial^4 \eta}{\partial \xi^4} - \lambda_s^2\frac{\partial^6 \eta}{\partial \xi^6} + \frac{\partial^2 \eta}{\partial \tau^2} + 2\beta^{\frac{1}{2}}\left(\frac{\gamma}{1+\gamma}\right)U_{avg}\frac{\partial^2 \eta}{\partial \xi \partial \tau} + \left(\frac{\gamma}{1+\gamma}\right)^2 U_{avg}^2\frac{\partial^2 \eta}{\partial \xi^2} + \psi\lambda_m^2\frac{\partial^6 \eta}{\partial \xi^4 \partial \tau^2} = 0 \tag{36}$$

The dimensionless equation by considering the nonlocal continuum theory and slip condition is as follows:

$$\frac{\partial^4 \eta}{\partial \xi^4} + \frac{\partial^2 \eta}{\partial \tau^2} + 2\beta^{\frac{1}{2}}\left(\frac{\gamma}{1+\gamma}\right)U_{avg}\frac{\partial^2 \eta}{\partial \xi \partial \tau} + \left(\frac{\gamma}{1+\gamma}\right)^2 U_{avg}^2\frac{\partial^2 \eta}{\partial \xi^2} - \phi^2\left(\frac{\partial^4 \eta}{\partial \xi^2 \partial \tau^2} + 2\beta^{\frac{1}{2}}\left(\frac{\gamma}{1+\gamma}\right)U_{avg}\frac{\partial^4 \eta}{\partial \xi^3 \partial \tau} + \left(\frac{\gamma}{1+\gamma}\right)^2 U_{avg}^2\frac{\partial^4 \eta}{\partial \xi^4}\right) = 0 \tag{37}$$

To the authors' knowledge, two last equations are innovative analytical approaches to take into account a 1D coupled FSI equation by considering the size effects of nano-flow and nano-structure simultaneously. Based on Askes and Aifantis [50], the results predicted by the strain/inertia gradient theory are in good agreement with those obtained by MD simulations; moreover, they

would reveal that strain/inertia gradient model for dynamical analysis of nano-tubes would be more reliable than other continuum theories.

4. Approximate solution

In order to solve the FSI equation, to calculate the CNT complex-valued eigen-frequencies, and to extract the divergence instability conditions, we use Galerkin's approximate solution method. This is approximate because of the finite number of terms utilized in the series solution expansion. Let:

$$\eta(\xi,\tau) \cong \sum_{n=1}^{N} \Phi_n(\xi) q_n(\tau). \tag{38}$$

where $q_n(\tau)$ are the generalized coordinate of the discretized system and $\Phi_n(\xi)$ are the comparison functions here, the eigen-functions of a beam with the same boundary conditions but no interaction between the fluid and structure. It is presumed that the series could be truncated at a suitably high value of n. It is noted that in this approximate method we need to choose comparison functions that satisfy the essential and natural boundary conditions of a CNT. In this work, we study the first divergence-type stability of a pinned–pinned CNT and the essential and natural boundary conditions for a simply-supported beam are as follows:

$$\eta(\xi,\tau) = 0 \text{ and } \frac{\partial^2 \eta}{\partial \xi^2} = 0 \quad \text{at } \xi = 0,1 \tag{39}$$

for this type of boundary condition, $\Phi_n(\xi)$ are considered as:

$$\Phi_n(\xi) = \sin(n\pi\xi) \tag{40}$$

We assume the generalized coordinates $q_n(\tau)$, $n = 1, 2, \ldots, N$ vary as simple harmonic motions (SHMs) for a free vibration response:

$$q_n(\tau) = Q_n \exp(s_n \tau) \tag{41}$$

where Q_n is constant amplitude of nth generalized coordinate of CNT free vibrations and s_n denotes the nth mode complex-valued eigen-frequency, whose real part shows the decaying rate in the nth mode (modal equivalent viscous damping) and the imaginary part show the nth modal damped natural frequency of the nano-beam.

4.1. Discritization

In this subsection, we use Galerkin weighted-residual technique for simply supported beam, and using dimensional equations. In this approximate method, we use the main governing differential equations of motion to compute the residue. For this purpose we start discritizing by choosing one generalized coordinate. We substitute the approximate function of $\eta(\xi,\tau)$ by $\sin(\pi\xi) \times q_1(\tau)$, to the fundamental differential Eq. (36) and Eq. (37) to calculate the residual. Then we multiply this residual by a weight function that is called test function. Herein, the comparison and the weight functions are the same and are selected as the first mode eigen-function ($\sin(\xi\pi)$). The resulting weighted residual is then integrated over the domain of the structure. This integrated weighted residual is then set to zero. It means that the error in the subspace spanned by trial functions is nullified and only the residual error orthgonal to this subspace would remain. This residual could have components in the complementary subspace of exact solution not spanned by the information subspace. The trial eigen-functions play the role of basis functions that span the complementary space of the infinite-dimensional space spanning exact solution. Consequently, the resulting discretized governing equations are as follows.

Strain/inertia gradient:

$$\left(\pi^4 - \pi^2\left(\frac{\gamma}{1+\gamma}\right)^2 U_{avg}^2 + \pi^6 \lambda_s^2\right)\frac{1}{2} q_1(\tau) + \frac{1}{2}\left(\pi^4 \lambda_m^2 \psi + 1\right)\ddot{q}_1(\tau) = 0$$

Nonlocal Eringen:

$$\left(\pi^4 - \pi^2\left(\frac{\gamma}{1+\gamma}\right)^2 U_{avg}^2 - \pi^4 \phi^2\left(\frac{\gamma}{1+\gamma}\right)^2 U_{avg}^2\right)\frac{1}{2} q_1(\tau) + \frac{1}{2}(\phi^2\pi^2 + 1)\ddot{q}_1\ (\tau) = 0 \tag{43}$$

The coefficient of $q_1(\tau)$, is denoting the sum of elastic stiffness and geometric stiffness parameters and the coefficient of $\ddot{q}_1(\tau)$ is representing the equivalent mass parameter.

4.2. Divergence analysis by novel coupled FSI equation

In this subsection, we arrange for a solution to discover the critical flow velocity at which the first divergence instability could occur by utilizing the developed coupled FSI equation in this article. Herein, we consider the effect of investigating slip velocity at the wall of CNT for different values of *Kn* numbers as well as the size effects of nano-structure via strain/inertia gradient and nonlocal continuum theories. According to Paidoussis [31], if the equivalent stiffness of a system can become zero for some critical value of fluid flow velocity, then the overall stiffness of the system vanishes which signifies that the divergence instability has occurred in the system. According to Eqs. (42) and (43), the equivalent stiffness, which is the addition of the flexural stiffness and geometric stiffness due to centrifugal effect of fluid velocity, for a pinned–pinned CNT conveying fluid are as follows:

Strain/inertia gradient:

$$K_{eq} = \pi^4 - \pi^2\left(\frac{\gamma}{1+\gamma}\right)^2 U_{avg}^2 + \pi^6 \lambda_s^2 \tag{44}$$

Nonlocal Eringen:

$$K_{eq} = \pi^4 - \pi^2\left(\frac{\gamma}{1+\gamma}\right)^2 U_{avg}^2 - \pi^4 \phi^2\left(\frac{\gamma}{1+\gamma}\right)^2 U_{avg}^2 \tag{45}$$

If we consider K_{eq} from Eq. (44) equal to zero, then we can calculate the first-mode critical flow velocity of the divergence-type instability by considering the strain/inertia gradient theory as:

$$U_{avg} = \pi\left(\frac{1+\gamma}{\gamma}\right)\sqrt{\pi^2 \lambda_s^2 + 1} \tag{46}$$

In addition, the first-mode critical flow velocity of the divergence-type instability by investigating the nonlocal continuum theory is as follows:

$$U_{avg} = \pi\left(\frac{1+\gamma}{\gamma}\right)\sqrt{\frac{1}{\pi^2 \phi^2 + 1}} \tag{47}$$

We conclude from Eqs. (46) and (47) that the first-mode critical average flow velocity would depend on *Kn* through the parameter γ and it would also depend on the size effect of nano-structure with λ_s and ϕ due to considering strain/inertia gradient and nonlocal theories.

5. Results and discussion

In this section, we utilize the approximate solution of Galerkin for simulating numerically the behavior of fluid passing through the nano-pipe. We may consider the material and geometrical properties of nano-tube as follows: CNT Young's modulus $E = 1$

TPa; thickness $h = 0.1$ nm; inner radius $R_i = 0.2$ nm; CNT mass density $\rho_{CNT} = 2.3\ \mathrm{g\ cm^{-3}}$; mass density of acetone $\rho_{ace} = 0.79\ \mathrm{g\ cm^{-3}}$ and mass density of air $\rho_{air} = 0.001169\ \mathrm{g\ cm^{-3}}$. In the numerical simulations, we utilized 1D basis function space to analyze only the first-mode divergence stability of CNT conveying fluid by the novel governing differential Eqs. (36) and (37).

5.1. Validation by no-slip condition formulation

In this subsection, we compare our numerical results with those of Paidoussis [31]. Since Paidoussis [31] investigates the plug flow theory, we need to substitute the coefficient $\gamma/(1+\gamma)$ by one in Eq. (24) and then discretize the equation of motion for validation. Fig. 3 shows how the imaginary parts of the fundamental eigen-frequency of a pipe would change for various values of average flow velocity of acetone, through a pinned–pinned pipe. In this case, the average flow velocity is assumed to be based on classical Navier–Stokes' continuum mechanics. We observe from this figure that as the mean flow velocity would increase from zero to a critical value, the resonant frequencies approach zero. For critical flow velocities, the resonant frequencies become zero; consequently, the pipe stiffness would disappear, and the divergence or column buckling mode occurs. As we observe from Fig. 3 we could see that the dimensionless mean critical flow velocity for the first-mode divergence would be equal to π, as we would expect from the observations of Paidoussis [31].

5.2. Effect of Kn on the divergence-type stability

In this subsection, we investigate the size effect of nano-flow with a nonzero *Kn* on the dynamic response of a nano-pipe conveying a liquid, herein, acetone as well as a gas, herein, air. According to Rashidi et al. [23] the range of *Kn* could vary from 0.001 to 0.01 for a liquid nano-flow and 0.001 to 2 for a gas nano-flow in slip flow regime. Table 1 discloses the dependency of dimensionless critical flow velocity to the diverse values of *Kn* as well as compares different models. By comparing the values of critical flow velocities for different *Kn*s, we might notice that the results of the innovative coupled FSI model developed here would seem drastically different from those of other FSI models, which is based on a plug flow theory as well as a velocity correction factor for considering the slip condition, as developed in [25]. Considering the slip velocity and coupled Eq. (24) could lead to appreciable effects on the general dynamic response of the CNT conveying nano-flow. For *Kn* equal to 0.001 (the threshold value of *Kn* for having a slip regime), the

Table 1
Variation of the first-mode dimensionless mean critical flow velocity against the variation of *Kn* for three different models including slip condition.

Kn	Dimensionless mean critical flow velocity (U_{avg})		
	Present model	Polard's model[a]	Roohi's model[b]
0	–	π	π
0.001	135.76π	0.992π	0.993π
0.005	28.06π	0.963π	0.965π
0.01	14.60π	0.927π	0.931π
0.05	3.83π	0.712π	0.702π
0.1	2.54π	0.549π	0.495π
0.5	1.40π	0.187π	0.105π
1	1.27π	0.099π	0.061π
1.5	1.23π	0.066π	0.049π
2	1.20π	0.050π	0.043π

[a] Polard's model for viscosity: $Cr(Kn) = \frac{1}{1+\frac{\sigma_M}{2-\sigma_v}0.89Kn+4.7Kn^2}$
[b] Roohi's model for viscosity: $Cr(Kn) = \frac{1}{1+\frac{\sigma_M}{2-\sigma_v}0.75Kn+19.98Kn^2}$.

dimensionless critical flow velocity would be about 140 times greater than that of predicted by Paidoussis [31], which is equal to π. Table 1 illustrates that the first-mode divergence instability phenomena might happen at a higher value of critical flow velocity. It means that coupled FSI model in this article predicts that pipe conveying nano-flow would lose its stability remarkably later than that predicted by continuum plug flow theory, and that plug flow theory complemented with the slip condition at the CNT walls such as Kaviani and Mirdamadi's model [25]. In that model, they used two different viscosity models of Roohi and Polard [25]. Furthermore, we observe from Table 1 that the divergence phenomena might happen in a lower critical flow velocity, for a higher *Kn*.

Fig. 4 illustrates the first-mode divergence instability and the imaginary parts of fundamental eigen-frequencies of pinned–pinned nano-tubes conveying acetone, for four different models. When the natural frequencies reduce to zero, the system loses stability by divergence and the corresponding flow velocity is defined as the critical flow velocity. This figure, which is drawn by considering the different values of dimensionless mean flow velocities and eigen-frequencies and the maximum value of *Kn* for a liquid nano-flow ($Kn = 0.01$), could reveal that the present model predicts the first-mode divergence instability would occur remarkably later than that predicted by continuum plug flow theory. Besides, Kaviani and Mirdamadi's model [25], which is based on defining the velocity correction factor (VCF), as well as Roohi and Polard's vis-

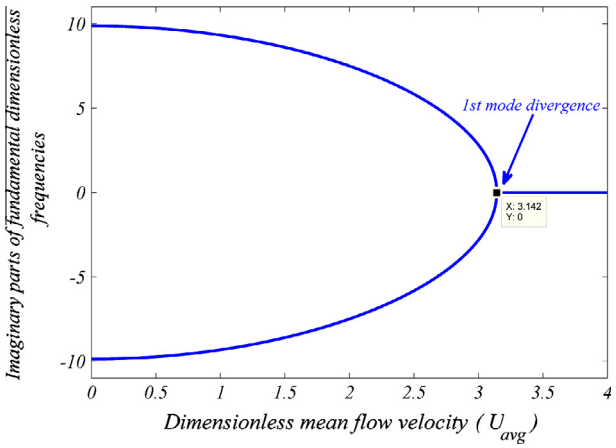

Fig. 3. Imaginary parts of dimensionless fundamental eigen-frequencies of pinned–pinned nano-tube against dimensionless mean flow velocity for acetone considering plug flow theory.

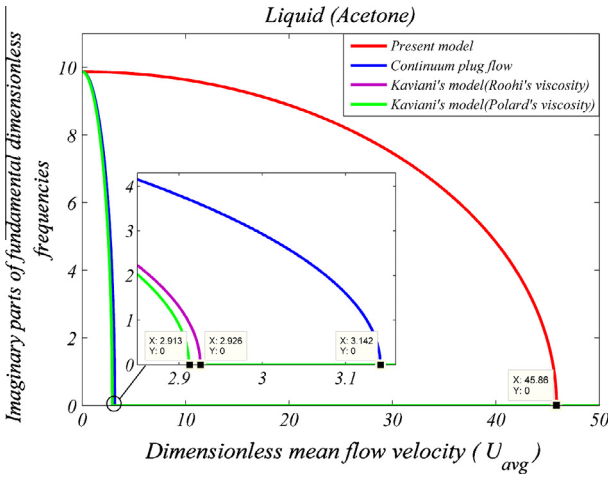

Fig. 4. Imaginary parts of dimensionless fundamental eigen-frequencies of pinned–pinned nano-tube conveying acetone, against dimensionless mean flow velocity for continuum plug flow and three models based on slip condition with maximum value of *Kn* for liquid nano-flow ($Kn = 0.01$).

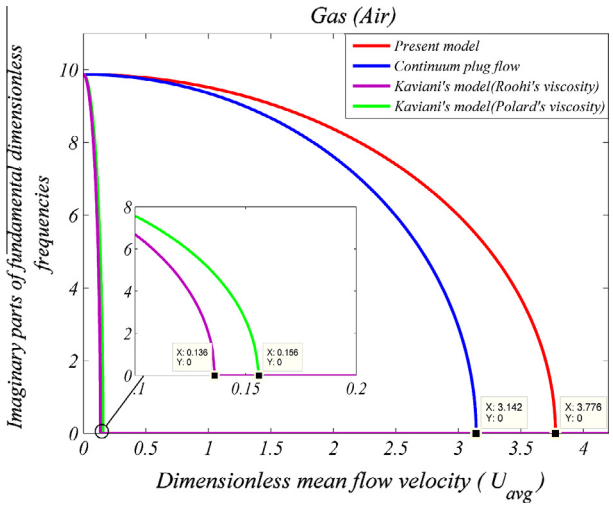

Fig. 5. Imaginary parts of dimensionless fundamental eigen-frequencies of pinned–pinned nano-tube conveying air, against dimensionless mean flow velocity for continuum plug flow and three models based on slip condition with maximum value of Kn for gas nano-flow ($Kn = 2$).

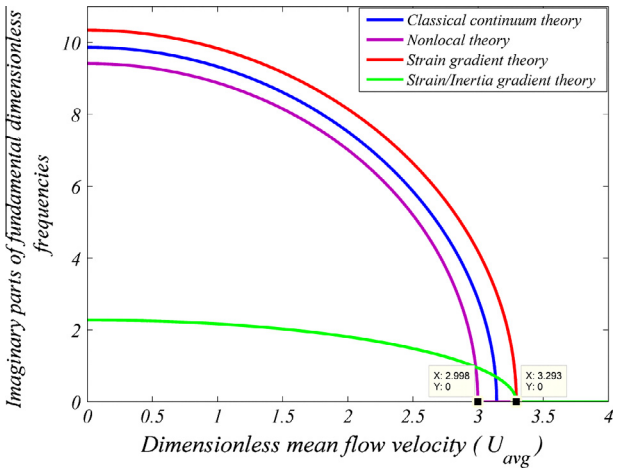

Fig. 6. Imaginary parts of dimensionless fundamental eigen-frequencies of pinned–pinned nano-tube conveying acetone, against dimensionless mean flow velocity for classical continuum theory and three models based on size-dependent continuum theories with maximum value of dimensionless characteristic lengths corresponding to the strain gradient ($\lambda_s = 0.1$), inertia gradient ($\lambda_m = 10\lambda_s$), and stress gradient ($\phi = 0.1$), without considering slip regime.

cosity models disclose that considering the slip boundary condition would advance the first-mode flow instability. Due to the fine differences, in Fig. 4 we depict the magnified parts around the first-mode divergence instability for the models discussed in [25]. In this figure, we observe that for the given value of Kn ($Kn = 0.01$), Polard's model predicts that the first-mode divergence instability could occur a little sooner than that predicted by Roohi's model.

Fig. 5 shows the same phenomena and results for a pinned–pinned nano-tube conveying gas, herein, air by considering a continuum plug flow theory and the other three models based on slip boundary condition for Kn equal to 2, which is the highest acceptable value for a slip regime of gas nano-flow. According to this figure, we observe again that our innovative model proposes a higher value for the critical flow velocity. However, for a gas nano-flow the critical flow velocity is closer to that of a plug flow theory, in comparison with liquid nano-flow. In addition, for a gas nano-flow, Roohi's model predicts that the first-mode divergence instability could occur a little sooner than that predicted by Polard's viscosity model but there is a little difference between Roohi and Polard's models.

5.3. Effects of size-dependent continuum theories on the divergence-type stability

In this subsection, we consider the effect of size-dependent continuum theories such as strain/inertia gradient and nonlocal continuum theories on the vibrational behavior of carbon nanotubes conveying fluid in a continuum plug flow regime. Before going to the details of figures, we ought to discuss the range of length scales, l_m, l_s and l which are respectively the characteristic lengths in relation to the inertia gradients, strain gradient and stress gradient (nonlocal theory). According to Askes and Aifantis [50] large range of values for these coefficients are possible. In our studies we use $l_s = l = 0.0355$ nm and $l_m = 10l_s$ for CNT (20,20) according to Askes and Aifantis [50]. In our work the length of the beam is in a nano-scale and is considered to be $L = 2R_i$ ($L = 0.4$ nm), consequently, the maximum values of dimensionless parameters λ_s and ϕ are 0.1.

Fig. 6 illustrates the first-mode divergence instability of pinned–pinned nano-tube conveying fluid for four different theories; namely, the strain/inertia gradient theory, the nonlocal theory, the classical continuum theory, and the strain gradient theory where the inertia gradient is ignored ($l_m = 0$ or $\lambda_m = 0$). Furthermore, we consider the maximum values for λ_s and ϕ which are 0.1 and $\lambda_m = 10\lambda_s$ for strain/inertia gradient theory. When the dimensionless mean flow velocity is equal to zero ($U_{avg} = 0$) the natural frequency predicted by the present strain gradient theory is greater than that predicted by the classical continuum theory as opposed to the natural frequency predicted by the nonlocal continuum theory which is smaller in comparison with the value predicted by the classical theory. The natural frequency predicted by strain/inertia gradient theory is drastically smaller in comparison with the three mentioned theories. For pipes with supported ends, the natural frequencies are diminished with increasing flow velocities. As we would observed from Fig. 6 strain and strain/inertia gradient theories predicted the same dimensionless mean critical flow velocity, which is greater than that predicted by classical continuum theory as we would observe from Eq. (46). It should be mentioned that these theories propose that pipe conveying fluid remains more stable in contrast with classical theories. However, as we would observe from Eq. (47) the nonlocal continuum theory suggests that pipe conveying fluid loses its stability sooner and the critical value is smaller than that of classical theory which is π.

5.4. Simultaneous effects of size-dependent continuum theories and Kn

We would analyze in this section small-scale effects on both elastic structure and fluid dynamic responses of CNT under liquid and gas nano-flow. Fig. 7 shows the vibration frequency of a CNT conveying fluid, herein, acetone. The frequency for the situations where characteristic lengths correspond to the highest values of $\lambda_s = \phi = 0.1$, $\lambda_m = 10\lambda_s$ and $Kn = 0.01$ for representing size-dependent effects, as well as the values of $\lambda_s = \phi = \lambda_m = 0$ for classical continuum theory with plug fluid flow. By considering the present model for investigating the size effects of nano-flow and nano-structure, the value of dimensionless mean critical flow velocity of the first-mode divergence would be remarkably greater. When we use the innovative 1D FSI equation by considering the slip regime at the CNT walls and strain/inertia or strain gradient theories, the amount of increase in the critical flow velocity would be greater in comparison with the situation where we investigate the effect of each of the size-dependent continuum theories and the Kn, separately. In fact, the superposition would not govern. Since the val-

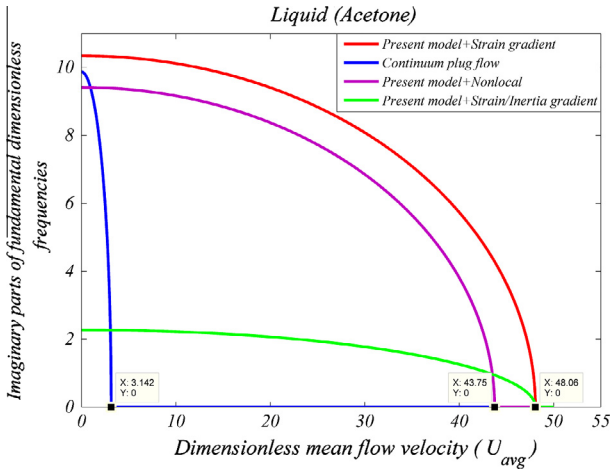

Fig. 7. Imaginary parts of dimensionless fundamental eigen-frequencies of pinned–pinned nano-tube conveying acetone, against dimensionless mean flow velocity for continuum plug flow theory and three models based on size-dependent continuum theories with maximum value of dimensionless characteristic lengths corresponding to the strain gradient ($\lambda_s = 0.1$), inertia gradient ($\lambda_m = 10\lambda_s$), and stress gradient ($\phi = 0.1$) including slip flow regime with maximum value of *Kn* for liquid nano-flow (*Kn* = 0.01).

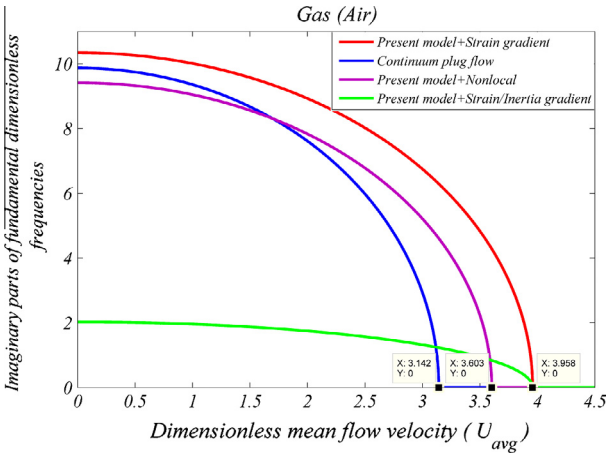

Fig. 8. Imaginary parts of dimensionless fundamental eigen-frequencies of pinned–pinned nano-tube conveying acetone, against dimensionless mean flow velocity for continuum plug flow theory and three models based on size-dependent continuum theories with maximum value of dimensionless characteristic lengths in relation to strain gradient ($\lambda_s = 0.1$), inertia gradient ($\lambda_m = 10\lambda_s$), and stress gradient ($\phi = 0.1$) including slip flow regime with maximum value of *Kn* for gas nano-flow (*Kn* = 2).

ues of increase in the first-mode is not equal to the effect of the values of increase for two superimposed cases. For example, in the first-mode the amount of increase due to slip regime (*Kn* = 0.01) and size-dependent continuum theories ($\lambda_s = \phi = 0.1, \lambda_m = 10\lambda_s$) are respectively, 42.72 and 0.151. The superposition of these two values is not equal to the amount of increase when we consider two effects superimposed, which is 44.92 ($42.72 + 0.151 \neq 44.92$). We may conclude that there should not be a linear relationship between the effects of these dimensionless parameters. The nonlocal continuum theory would predict reduction in the dimensionless mean critical flow velocity; nevertheless, by studying the simultaneous effects of nonlocal and slip regime, the critical value of flow velocity could increase significantly and a pinned–pinned system would lose its stability strikingly delayed. However, we may only declare, in a liquid nano-flow, that the *Kn* would be playing a more important role then the dimensionless nonlocal parameter. Indeed, *Kn* completely nullifies the effect of nonlocal parameter in the reducing the critical velocities.

Fig. 8 shows the vibration frequency of a CNT conveying gas, herein, the air for the situations that the characteristic parameters are considered with the highest value ($\lambda_s = \phi = 0.1$, $\lambda_m = 10\lambda_s$ and *Kn* = 2), as well as for a classical continuum theory with plug fluid flow. When we study the effects of slip regime and strain/inertia or strain gradient theory simultaneously the amount of increase in the mean critical flow velocity is 0.816, which is greater than those values of increase by considering the slip regime and strain gradient theory, which are respectively, 0.634 and 0.151. We may conclude that the characteristic lengths correspond to the strain/inertia gradient theory (λ_m, λ_s) could cancel out some effect of *Kn*. It should be better to say that by increasing the value of *Kn* the critical value of mean flow velocity approaches the value predicted by the model based on standard elasticity theory and plug flow but the strain gradient theory opposes and predicts a greater value for the critical velocity as well as the system remains more stable. In the case of nonlocal theory with slip flow regime, the nonlocal parameter causes the critical value becomes closer to that of predicted by plug flow theory. It should be better to say that by considering only the *Kn* the amount of increase in the critical flow velocity is 0.634 and by investigating the simultaneous effects this amount is equal to 0.461. According to the discussion and the results of Fig. 8 we could easily guess that in a gas nano-flow, *Kn* has more contribution in the variation of critical velocity than nonlocal parameter.

6. Conclusions

In this study, we investigated the effect of viscosity of a fluid flow in a channel and the interaction between the fluid and structure. We reappraised the governing differential equation of pipe conveying viscous fluid derived and used by several researchers during the last decade. In this article, we utilized the prominent principles of fluid mechanics such as Navier–Stokes' equation as well as several valuable references in the field of FSI to reveal that the viscosity of the fluid flow could not appear explicitly in the equation of motion of a pipe conveying fluid. Accordingly, we proposed an innovative model for the 1D coupled vibrations of carbon nano-tubes (CNTs) conveying fluid using the slip regime of fluid flow at the walls of CNT and some size-dependent continuum theories. The first-mode dimensionless mean critical flow velocity predicted by the innovative model for considering the slip regime with classical continuum theories, which would show a considerable increase, as opposed to those for plug flow theory without considering slip boundary condition and even with this effect. Therefore, this innovative model, presented in this article would propose that CNT conveying nano-flow could remain more stable, i.e., the critical average velocity of the fluid flow at which the first-mode divergence instability would occur, could be extremely greater in comparison with that of predicted by a plug flow theory. In addition, a CNT conveying liquid nano-flow could remain more stable in contrast with a gas nano-flow. Moreover, as the *Kn* number would increase, this innovative model would approach the plug flow theory and the critical flow velocity predicted by both models would become the same. In the case of studying the effect of size-dependent continuum theories, we would observe that the natural frequency predicted by the strain gradient theory is greater than that predicted by the classical continuum theory, as opposed to the natural frequency predicted by the nonlocal continuum theory, which is smaller in comparison with the value predicted by the classical theory. The natural frequency predicted by strain/inertia gradient theory is drastically smaller in comparison with the three mentioned theories. Besides, the dimensionless mean critical flow velocity predicted by strain/inertia or strain gradient theories

would be greater than that predicted by classical continuum theory as opposed to the value suggested by nonlocal theory which is smaller than that predicted by classical theory. By considering the *Kn* and size-dependent continuum theories simultaneously, we may conclude that *Kn* has more contribution in the variation of critical velocity than size-dependent parameters. Moreover, in a liquid nano-flow we may declare that *Kn* thoroughly nullify the effect of nonlocal parameter and a pinned–pinned system remains considerably stable in contrast with plug flow theory. For a gas nano-flow where the value of *Kn* is increasing the parameters with respect to the strain gradient theory opposes the effect of *Kn* and increase the value of dimensionless critical flow velocity; however, the nonlocal parameter makes the critical value closer to that predicted by FSI equation based on classical theory and plug flow.

References

[1] E.T. Thostenson, Z. Ren, T.W. Chou, Compos. Sci. Technol. 61 (2001) 1899–1912.
[2] Y. Gao, Y. Bando, Nature 415 (2002) 599.
[3] N. Moldovan, K.H. Kim, H.D. Espinosa, J. Microelectromech. Syst. 15 (2006) 204–213.
[4] S. Joseph, N.R. Aluru, Nano. Lett. 8 (2008) 452–458.
[5] R.E. Tuzun, D.W. Noid, B.G. Sumpter, R.C. Merkle, Nanotechnology 7 (1996) 241–246.
[6] M. Amabili, F. Pellicano, M.P. Paidoussis, Comput. Struct. 80 (2002) 899–906.
[7] J. Yoon, C.Q. Ru, A. Mioduchowski, Compos. Sci. Technol. 65 (2005) 1326–1336.
[8] T. Natsuki, Q.Q. Ni, M. Endo, J. Appl. Phys. 101 (2007) 034319.
[9] L. Wang, Q. Ni, M. Li, Com. Mater. Sci. 44 (2008) 821–825.
[10] W. Xia, L. Wang, L. Yin, Int. J. Eng. Sci. 48 (2010) 2044–2053.
[11] L. Wang, N. Qiao, Comput. Struct. 86 (2008) 133–139.
[12] N. Khosravian, H. Rafii-Tabar, J. Phys. D: Appl. Phys. 40 (2007) 7046–7052.
[13] L. Wang, Q. Ni, Mech. Res. Commun. 36 (2009) 833–837.
[14] H.L. Lee, W.J. Chang, Physica E 41 (2009) 529–532.
[15] P. Soltani, M.M. Taherian, A. Farshidianfar, J. Phys. D: Appl. Phys. 43 (2010) 425401.
[16] Z. Khoddami, A. Ghorbanpour Arani, R. Kolahchi, S. Amir, M.R. Bagheri, Compos. Part B: Eng. 45 (2013) 423–432.
[17] H.L. Lee, W.J. Chang, Physica E 41 (2009) 529–532.
[18] Y. Zhen, B. Fang, Comp. Mater. Sci. 49 (2010) 276–282.
[19] H. Jannesari, M.D. Emami, H. Karimpour, Phys. Lett. A 376 (2012) 1137–1145.
[20] L.L. Ke, Y.S. Wang, Physica E 43 (2011) 1031–1039.
[21] L. Wang, Comp. Mater. Sci. 49 (2010) 761–766.
[22] L. Wang, Physica E 43 (2010) 437–439.
[23] V. Rashidi, H.R. Mirdamadi, E. Shirani, Comput. Mater. Sci. 51 (2012) 347–352.
[24] M. Mirramezani, H.R. Mirdamadi, Arch. Appl. Mech. 82 (2012) 879–890.
[25] F. Kaviani, H.R. Mirdamadi, Comput. Struct. 116 (2013) 75–87.
[26] M. Mirramezani, H.R. Mirdamadi, Physica E 44 (2012) 2005–2015.
[27] F. Kaviani, H.R. Mirdamadi, Comput. Mater. Sci. 61 (2012) 270–277.
[28] M.R. Matin, H.R. Mirdamadi, M. Ghayour, Physica E 48 (2013) 85–95.
[29] M.P. Paidoussis, B.E. Laithier, J. Mech. Eng. Sci. 18 (1976) 210–220.
[30] F.M. White, Fluid Mechanics, McGraw-Hill, New York, 1982.
[31] M.P. Paidoussis, Fluid–Structure Interactions: Slender Structures and Axial Flow, vol. 1, Academic Press, London, 1998.
[32] M.P. Paidoussis, J. Fluid. Struct. 20 (2005) 871–890.
[33] M.P. Paidoussis, J. Sound. Vib. 310 (2008) 462–492.
[34] C.Q. Guoa, C.H. Zhanga, M.P. Paidoussis, J. Fluid. Struct. 26 (2010) 793–803.
[35] T.B. Benjamin, Proc. R. Soc. A 261 (1961) 457–486.
[36] G. Karniadakis, A. Beskok, N. Aluru, Microflows and Nanoflows: Fundamentals and Simulation, Springer, New York, 2005.
[37] A. Beskok, G.E. Karniadakis, Microscale. Therm. Eng. 3 (1999) 43–77.
[38] H. Shokouhmand, A.H.M. Isfahani, E. Shirani, Int. Commun. Heat Mass. 37 (2010) 890–894.
[39] R.D. Mindlin, Int. J. Solids. Struct. 1 (1965) 417–438.
[40] N.A. Fleck, J.W. Hutchinson, J. Mech. Phys. Solids. 49 (2001) 2245–2271.
[41] H. Askes, E.C. Aifantis, Int. J. Solids. Struct. 48 (2011) 1962–1990.
[42] L. Wang, J. Vib. Control. 18 (2012) 313–320.
[43] A.C. Eringen, J. Appl. Phys. 54 (1983) 4703;, http://dx.doi.org/10.1063/1.332803.
[44] J.N. Reddy, S.D. Pang, J. Appl. Phys. 103 (2008) 023511.
[45] A. Tounsi, H. Heireche, E.A.A. Bedia, J. Phys. 105 (2009) 126105.
[46] L. Wang, Physica E 41 (2009) 1835–1840.
[47] C.W. Lim, Appl. Math. Mech. 31 (2010) 37–54.
[48] C.W. Lim, Y. Yang, J. Comput. Theor. Nanosci. 7 (2010) 988–995.
[49] L. Wang, Physica E 44 (2011) 25–28.
[50] H. Askes, E.C. Aifantis, Gradient elasticity and flexural wave dispersion in carbon nano-tubes, Phys. Rev. B 80 (2009) 195412.